

TJ4DRadSet: A 4D Radar Dataset for Autonomous Driving

Lianqing Zheng¹, Zhixiong Ma^{1,*}, Xichan Zhu¹, Bin Tan¹, Sen Li¹, Kai Long¹, Weiqi Sun¹, Sihan Chen¹, Lu Zhang¹, Mengyue Wan¹, Libo Huang², Jie Bai^{2,*}

Abstract— The new generation of 4D high-resolution imaging radar provides not only a huge amount of point cloud but also additional elevation measurement, which has a great potential of 3D sensing in autonomous driving. In this paper, we introduce an autonomous driving dataset named TJ4DRadSet, including multi-modal sensors that are 4D radar, lidar, camera and GNSS, with about 40K frames in total. 7757 frames within 44 consecutive sequences in various driving scenarios are well annotated with 3D bounding boxes and track id. We provide a 4D radar-based 3D object detection baseline for our dataset to demonstrate the effectiveness of deep learning methods for 4D radar point clouds.

I. INTRODUCTION

In recent years, autonomous driving technology [1] has received much attention. A high-level autonomous driving vehicle mainly consists of modules such as environment perception, road planning, and decision execution [2]. Among them, the perception module is the upstream module, whose performance directly affects the safety of the self-driving vehicle. At this stage, the perception module mainly uses sensors such as camera, lidar, and mmWave radar to obtain environmental information of different modes [3]. It is undeniable that the camera and lidar will fail to varying degrees when the self-driving vehicle is driven under harsh driving conditions such as rain, fog, and intense light. In contrast, mmWave radar is indispensable because of its strong robustness [4] and low price. Due to the low angular resolution, traditional mmWave radar is only used for blind-spot detection, collision warning, and other driving assistance functions. The emergence of 4D high-resolution imaging radar [5] makes up for this shortcoming, and we believe it is expected to become the main sensor in high-level autonomous driving. The four dimensions of 4D radar are range, azimuth, elevation, and Doppler velocity. Because of the high azimuth and elevation resolution, the 4D radar produces denser 3D point clouds with velocity information.

3D perception tasks are crucial in the environment perception module, such as 3D object detection and tracking. With the development of deep learning and artificial intelligence, more and more neural networks are being applied in 3D perception [6]. It is well known that the training of neural networks requires large-scale data. For 3D object detection task, the data collected by sensors are diverse and complex, which needs to cover many actual conditions. What's more, the ground truth of data needs to be accurate for supervised learning to ensure the trained network is valid. Compared with camera and lidar, few autonomous driving datasets contain 4D radar, which limits the research and

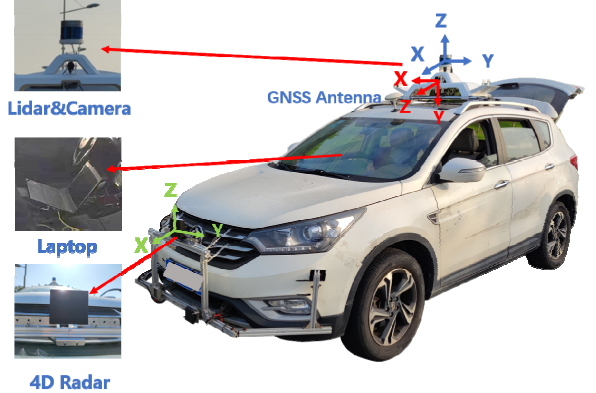


Figure 1. Data acquisition platform and coordinate system.

application of deep learning in the 4D radar point cloud. To fill this gap, we propose a 4D radar dataset for autonomous driving called TJ4DRadSet. Our data collection platform is shown in figure 1. The dataset contains multi-sensors, including 4D radar, camera, lidar, and GNSS. We hope that the dataset will facilitate the research of 4D radar-based perception algorithms. Our main contributions are listed as follows :

- We present a multi-modal dataset named TJ4DRadSet. It is an autonomous driving dataset containing 4D radar point cloud with continuous sequences and 3D annotations. In addition, the dataset also provides complete information for other sensors.
- TJ4DRadSet contains a total of 40K frames of synchronized data, where 7757 frames, 44 sequences with high-quality annotated 3D bounding boxes and track id. The 3D annotation system uses joint multi-sensor annotation and multi-round manual checks.
- TJ4DRadSet covers various road conditions, such as elevated roads, complex intersections, one-way roads, and urban roads. It also includes bad lighting conditions such as strong light and darkness. The dataset is suitable for developing 3D perception algorithms based on the 4D radar to facilitate its application in high-level autonomous driving.

¹Lianqing Zheng, Bin Tan, Sen Li{zhenglianqing, tanbin, lisen,}@tongji.edu.cn

TABLE I. CURRENT DRIVING RADAR DATASETS

| Dataset | Size | Radar Type | Other Modalities | 4D Radar Point Cloud | Object Detection | Object Tracking | 3D Annotations |
|--------------------------|--------|-----------------|------------------|----------------------|------------------|-----------------|----------------|
| Nuscenes[9] | Large | Low Resolution | Lidar&Camera | ✗ | ✓ | ✓ | ✓ |
| RADIATE[12] | Middle | Scanning | Lidar&Camera | ✗ | ✓ | ✓ | ✗ |
| MulRan[13] | Middle | Scanning | Lidar | ✗ | ✗ | ✗ | ✗ |
| RadarScenes[10] | Large | Low Resolution | Camera | ✗ | ✓ | ✓ | ✗ |
| RadarRobotCar[11] | Large | Scanning | Lidar&Camera | ✗ | ✗ | ✗ | ✗ |
| Astyx[14] | Small | High Resolution | Lidar&Camera | ✓ | ✓ | ✗ | ✓ |
| RADIaL[15] | Middle | High Resolution | Lidar&Camera | ✓ | ✓ | ✗ | ✗ |
| TJ4DRadSet (ours) | Middle | High Resolution | Lidar&Camera | ✓ | ✓ | ✓ | ✓ |

- Based on TJ4DRadSet, we provide a baseline for 4D radar-based 3D object detection. The results show that 4D radar has a promising potential for high level autonomous driving.

The paper is organized as follows: section II introduces some related work on other datasets. Section III describes our dataset in detail. In section IV, we perform the baseline result of 3D object detection based on 4D radar, and a brief conclusion and future work are presented in section V.

II. RELATED WORK

Deep learning technique is playing an increasing role in autonomous driving. It relies on a large amount of high-quality data. Therefore, more and more open dataset benchmarks have appeared in recent years, such as KITTI [7] and Waymo Open [8], which have contributed to the advancement of autonomous driving technology. With these benchmarks, we can evaluate the performance of different algorithms for various tasks.

MmWave radar has proven to be an effective sensor due to its robustness in all weather and low price. However, many datasets do not contain mmWave radar information, which limits the application of data-driven algorithms based on radar data. Since the nuScenes [9] dataset was released, some datasets with radar data started to appear. There is a growing interest in mmWave radar. The comparison of each dataset containing radar data is shown in Table I. Some datasets contain low-resolution FMCW radar point cloud, such as nuScenes, and RadarScence [10]. These point clouds lack elevation information for accurate 3D perception. Some datasets use scanning radar to collect data, such as RadarRobotCar [11], RADIATE [12], and MulRan [13]. These radar data are mainly interpreted as image data and lack Doppler velocity. For the new generation of 4D imaging radar, the 4D point cloud will be the primary output format, containing spatial and velocity information. Currently, Astyx [14] and RADIaL [15] include high-resolution radar point cloud. Astyx has only 500+ frames of point cloud data, which is too small and lacks of tracking information. RADIaL contains complete radar data, such as distance-Doppler maps, point clouds, etc. It only has 2D labeled boxes and “Car” label.

III. THE TJ4DRADSET DATASET

In this section, we introduce sensor parameters, sensor calibration, data collection and annotation, then provide statistical analysis and visualization.

A. Sensors

The TJ4DRadSet mainly contains 4D radar, lidar and camera. The sensor layout of the acquisition platform is shown in Figure 1. The camera and lidar are mounted on the roof bracket, and the 4D radar is installed in the middle of the front ventilation gride. The lidar can collect 360° of environmental information, while the camera and 4D radar capture the information in the FOV ahead, covering the forward driving view. The main parameters of each sensor are shown in Table II. In addition, the GNSS information is included and corrected by RTK to achieve high-precision positioning, which has the speed and location information of the ego vehicle.

B. Sensor Calibration

Multi-sensor calibration is the basis for perception algorithm. The process mainly consists of intrinsic parameters calibration, extrinsic calibration, and temporal alignment. The intrinsic parameters and distortion coefficients of the camera are calibrated by MATLAB Toolkit [16] and a checkerboard. The distortion coefficients are used for correction to obtain rectified images. The intrinsic parameters of 4D radar and lidar have been calibrated offline at the factory.

For extrinsic parameters calibration, it can be divided into two processes: camera and lidar extrinsic calibration, 4D radar and lidar extrinsic calibration. The extrinsic parameters of the camera and 4D radar can be obtained by performing matrix operations on the remaining two extrinsic parameters. The extrinsic parameters between the different sensors are represented as translation and rotation matrix. For camera and lidar extrinsic calibration, we use a checkerboard to perform 2D-3D alignment of the point cloud and image data to complete a rough calibration. Then, we manually fine-tune the extrinsic parameters by static objects such as trees and poles in the environment. For 4D radar and lidar extrinsic calibration, we consider it as 3D-3D point cloud alignment in space. Firstly, the distance between the two sensors is measured as a rough

TABLE II. SPECIFICATION OF THE TJ4DRADSET'S SENSOR SUITES

| Sensors | Parameters | | | Resolution | | | FPS |
|----------|------------|-----------|-----------|------------|---------|-----------|-----|
| | Range | Azimuth | Elevation | Range | Azimuth | Elevation | |
| Camera | | 1280px | 960px | | 66.5° | 94° | 30 |
| Lidar | 0.03m | 0.1°-0.4° | 0.33° | 120m | 360° | 40° | 10 |
| 4D Radar | 0.86m | <1° | <1° | 400m | 113° | 45° | 15 |

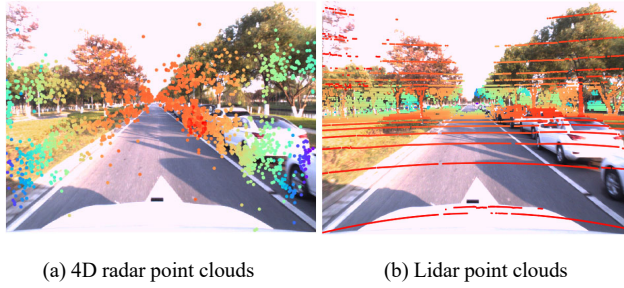


Figure 2. 4D radar and lidar point clouds projection.

translation parameter. Then extrinsic parameters are fine-tuned by using multiple angular reflectors in space.

All sensors work under ROS driver. Since each sensor runs at different frame rates, we align the data by using the arrival time of the data as the timestamp. The final 4D radar and lidar point clouds are projected into the image, as shown in Figure 2.

C. Data Collection and Annotation

TJ4DRadSet was collected from Suzhou, China, in the fourth quarter of 2021. Figure 3 records the location of the data collection. The dataset covers a wide range of driving conditions. Specifically, it includes various lighting conditions, such as normal lighting, bright light and darkness, and different road types, such as urban roads, elevated roads, industrial zones, etc. There are complex scenarios such as object-dense intersections, and simple scenarios such as one-way streets with a few objects. Our acquisition system is based on ROS operation and all sensor data are recorded in “rosbag” completely.

The ground truth annotation of the dataset mainly includes 3D bounding box, class and track id for each object. It is undeniable that lidar has a higher point cloud density than 4D radar at this stage, which provides a clearer description of the



Figure 3. Locations of the data collection.

objects shape. Therefore, our annotation system mainly relies on lidar point clouds and images for joint annotation. However, some objects that have few lidar points due to occlusion may still appear in 4D radar FOV because of the multipath effect, and we still label them. We finished the annotation manually and reviewed many rounds to ensure the quality of the dataset.

The 3D bounding box of each object includes center point (x,y,z), length, width, height (l,w,h), and orientation angle (yaw). In addition, we provide occlusion and truncation indicators. The dataset have eight classes (Car, Bus, Truck, Engineering Vehicle, Pedestrian, Motorcyclist, Cyclist, Tricyclist). In order to have a balanced label distribution and to improve the performance of networks, we map the “Bus” and “Engineering Vehicle” (large) as “Truck”, the “Motorcyclist” as “Cyclist”. The class of other objects is mapped as “Other Vehicle”. The original classes are retained and can be mapped as custom as needed. We assign a unique id to each object for tracking task. Finally, about 40K frames of synchronized data are extracted, 7757 frames of data are labeled.

D. Dataset Statistics

In this section, we perform some statistical analysis of the dataset. Figure 4(a) shows the number of objects for each class, with “Car” being the most numerous, followed by “Cyclist”. The amount of “Truck” and “Pedestrian” is approximately same. Figure 4(b) shows the speed distribution of the ego vehicle. The distribution of the point cloud density of lidar and 4D radar is shown in Figure 4(c)(d). We can see that the 4D radar point cloud is more sparse than the laser point cloud, but radar points contain more features, such as Doppler velocity. In addition, we also count the distribution of the distances and orientations of main classes, shown in Figure 5. Some typical scenarios are visualized in Figure 6.

IV. BASELINE EXPERIMENTS

In this section, we establish the baseline of 3D object detection based on 4D radar. To ensure the trained model is valid, we divide the dataset into training set and test set by sequence and keep the test set with good coverage. By this way, we get 5717 training samples and 2040 test samples.

The original annotation information is under the lidar coordinate system, and we transfer the labels to the 4D radar coordinate system through the lidar-radar extrinsic matrix. As shown in Figure 4(c), 4D radar has only 2000 to 3000 points per frame in most cases. Therefore, some of the existing networks are difficult to be applied directly to this sparse data format. In this paper, we use PointPillars [17] as the baseline algorithm because of its good adaptability and the trade-off in both speed and precision. To adapt the 4D radar data, we have

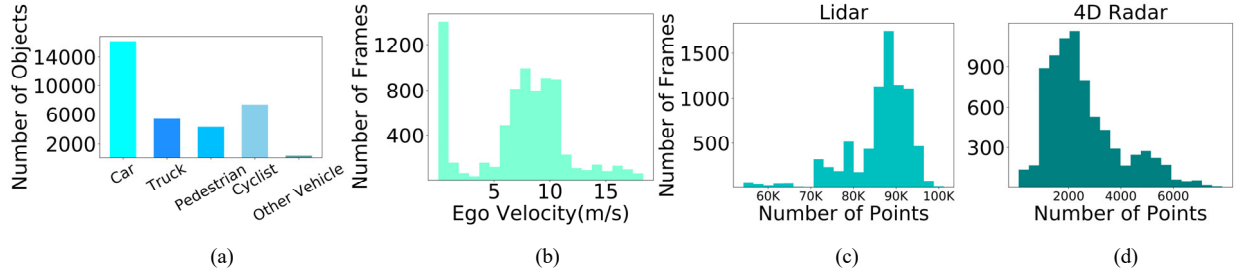


Figure 4. (a) Number of objects for each class. (b) Speed distribution of the ego vehicle. (c) Lidar point cloud density. (d) 4D radar point cloud density.

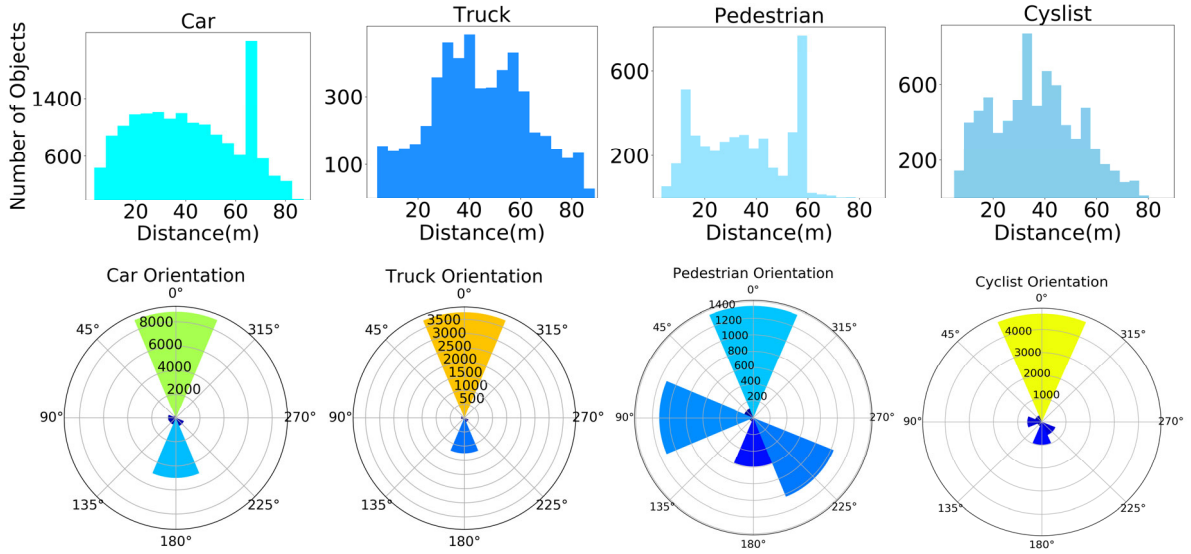


Figure 5. Distribution of the distances and orientations of “Car”, “Truck”, “Pedestrian” and “Cyclist”

TABLE III. BASELINE RESULTS

| Class | BEV-50m | | 3D-50m | | BEV-70m | | 3D-70m | |
|------------|---------|---------|--------|---------|---------|---------|--------|---------|
| | AP@0.5 | AP@0.25 | AP@0.5 | AP@0.25 | AP@0.5 | AP@0.25 | AP@0.5 | AP@0.25 |
| Car | 23.06 | 36.73 | 12.63 | 27.96 | 26.19 | 40.14 | 16.85 | 33.30 |
| Truck | 16.76 | 36.37 | 12.64 | 31.33 | 13.46 | 30.49 | 10.07 | 25.51 |
| Pedestrian | | 35.24 | | 27.64 | | 35.26 | | 27.19 |
| Cyclist | 21.62 | 40.26 | 18.34 | 38.42 | 21.38 | 39.80 | 17.70 | 38.20 |

partially modified the original configuration and retrained the model using TJ4DRadSet.

The detection range along the x-axis is set to 69.12m. We use 4 features of radar points for training and testing, which include spatial information (x,y,z) and Doppler velocity v. The Doppler velocity v is the absolute radial velocity after compensation by ego-motion. In terms of network parameters, we choose the size of the pillar to be (0.16m, 0.16m). We define the anchor size format as (l,w,h). The anchor sizes of “Car”, “Truck”, “Pedestrian”, “Cyclist” are listed as followed :(4.56m, 1.84m, 1.70m), (10.76m, 2.66m, 3.47m), (0.80m, 0.60m, 1.69m), (1.77m, 0.78m, 1.60m). To enhance the robustness of the network, we use data augmentations, including the world random rotation and random scaling. We use the Adam optimizer [18] to train the model for 70 epochs.

In the evaluation stage, we use the average precision (AP) to evaluate the detection results for each class. Table III shows the baseline results. For “Car”, “Truck”, and “Cyclist”, we use 0.5 and 0.25 IoU threshold to test. For “Pedestrian”, we only use 0.25 IoU threshold to evaluate. We denote the AP under these two thresholds as AP@0.5 and AP@0.25. We evaluate the model performance at different distances (50m and 70m) and different views(BEV, 3D).

From the results, we can see that 4D radar has potential in 3D perception. In BEV view, the average accuracy for all classes is over 30% at 0.25 IOU threshold. Although the baseline algorithm can achieve some results, there is still a lot of improvement potential. It is of great concern how to better extract 4D radar point cloud features and fuse information from other modalities.

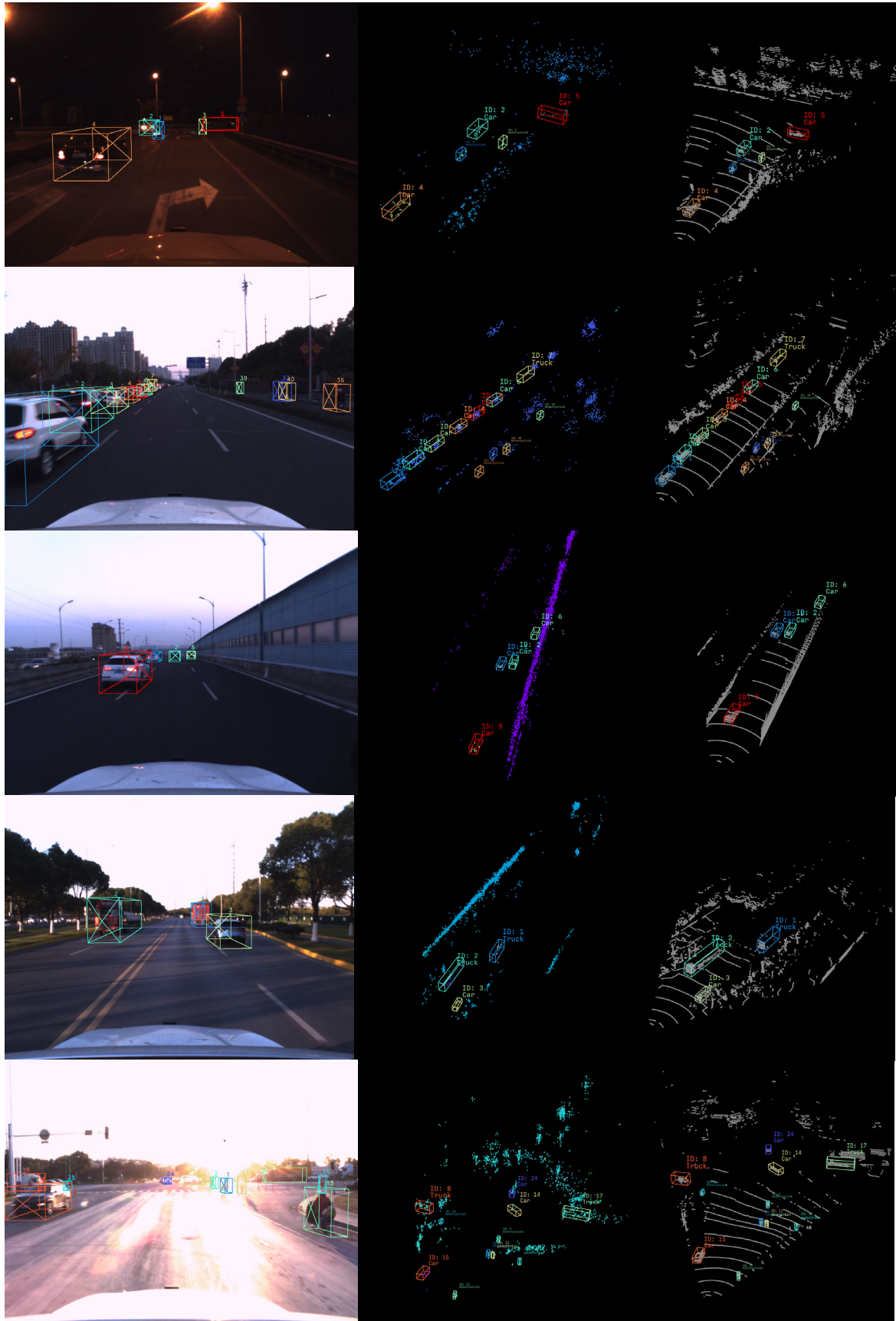


Figure 6. Visualization of typical samples of TJ4DRadSet.

V. CONCLUSION AND FUTURE WORK

In this paper, we introduce TJ4DRadSet, a multi-model autonomous driving dataset containing 4D radar point cloud. The dataset is used to study 4D radar-based 3D perception algorithms. We provide a detailed description of the dataset and conduct baseline experiments. In the future, we will further expand the dataset and research on fusion algorithms, point cloud enhancement and feature representation based on 4D radar.

REFERENCES

- [1] A. Agafonov and A. Yumaganov, “3D Objects Detection in an Autonomous Car Driving Problem,” in *2020 International Conference on Information Technology and Nanotechnology (ITNT)*, 2020, pp. 1-5.
- [2] X. Duan, H. Jiang, D. Tian, T. Zou, J. Zhou and Y. Cao, “V2I based environment perception for autonomous vehicles at intersections,” *China Communications*, vol. 18, no. 7, pp. 1-12, July 2021.
- [3] R. Ravindran, M. J. Santora and M. M. Jamali, “Multi-Object Detection and Tracking, Based on DNN, for Autonomous Vehicles: A Review,” *IEEE Sensors Journal*, vol. 21, no. 5, pp. 5668-5677, Mar. 2021.
- [4] S. Lee, Y. J. Yoon, J. E. Lee and S. C. Kim, “Human–vehicle classification using feature-based SVM in 77-GHz automotive FMCW radar,” *IET Radar, Sonar and Navigation*, vol. 11, no. 10, pp. 1589-1596, Aug. 2017.
- [5] S. Brisken, F. Ruf, F. Höhne, “Recent evolution of automotive imaging radar and its information content,” *IET Radar, Sonar and Navigation*, vol. 12, no. 10, pp. 1078-1081, Oct. 2018.
- [6] E. Arnold, O. Y. Al-Jarrah, M. Dianati, S. Fallah, D. Oxtoby and A. Mouzakitis, “A Survey on 3D Object Detection Methods for Autonomous Driving Applications,” *IEEE Transactions on Intelligent Transportation Systems*, vol. 20, no. 10, pp. 3782-3795, Oct. 2019.
- [7] A. Geiger, P. Lenz, C. Stiller, and R. Urtasun, “Vision meets robotics: The KITTI dataset,” *International Journal of Robotics Research*, vol. 32, no. 11, pp. 1231-1237, Sep. 2013.
- [8] P. Sun, H. Kretzschmar, X. Dotiwalla, A. Chouard, V. Patnaik, P. Tsui, J. Guo, Y. Zhou, Y. Chai, B. Caineet al., “Scalability in perception for autonomous driving: Waymo open dataset,” in *Proceedings of the IEEE/CVF Conference on Computer Vision and Pattern Recognition (CVPR)*, 2020, pp. 2446-2454.
- [9] H. Caesar, V. Bankiti, A. H. Lang, S. Vora, V. E. Liang, Q. Xu, A. Krishnan, Y. Pan, G. Baldan, and O. Beijbom, “nuscenes: A multimodal dataset for autonomous driving,” in *Proceedings of the IEEE/CVF Conference on Computer Vision and Pattern Recognition (CVPR)*, 2020, pp. 11621-11631.
- [10] O. Schumann et al., “RadarScenes: A Real-World Radar Point Cloud Data Set for Automotive Applications,” in *2021 IEEE 24th International Conference on Information Fusion (FUSION)*, 2021, pp. 1-8.
- [11] D. Barnes, M. Gadd, P. Murcett, P. Newman and I. Posner, “The Oxford Radar RobotCar Dataset: A Radar Extension to the Oxford RobotCar Dataset,” in *2020 IEEE International Conference on Robotics and Automation (ICRA)*, 2020, pp. 6433-6438.
- [12] M. Sheeny, E. De Pellegrin, S. Mukherjee, A. Ahrabian, S. Wang and A. Wallace, “RADIATE: A Radar Dataset for Automotive Perception in Bad Weather,” in *2021 IEEE International Conference on Robotics and Automation (ICRA)*, 2021, pp. 1-7.
- [13] G. Kim, Y. S. Park, Y. Cho, J. Jeong and A. Kim, “MulRan: Multimodal Range Dataset for Urban Place Recognition,” in *2020 IEEE International Conference on Robotics and Automation (ICRA)*, 2020, pp. 6246-6253.
- [14] M. Meyer and G. Kuschk, “Automotive Radar Dataset for Deep Learning Based 3D Object Detection,” in *2019 16th European Radar Conference (EuRAD)*, 2019, pp. 129-132.
- [15] J. Rebut, A. Ouaknine, W. Malik, P. Pérez, “Raw High-Definition Radar for Multi-Task Learning,” *arXiv preprint arXiv: 2112.10646*, 2021.
- [16] “Matlab camera calibration,” <https://www.mathworks.com/help/vision/ug/camera-calibration.html>, 2021.
- [17] A. H. Lang, S. Vora, H. Caesar, L. Zhou, J. Yang, and O. Beijbom, “Pointpillars: Fast encoders for object detection from point clouds,” in *Proceedings of the IEEE/CVF Conference on Computer Vision and Pattern Recognition (CVPR)*, 2019, pp. 12697-12705.
- [18] D. P. Kingma, J. Ba, “Adam: A Method for Stochastic Optimization”, *arXiv preprint arXiv: 1412.6980*, 2014.